Purdue University
Purdue e-Pubs

International Refrigeration and Air Conditioning Conference

School of Mechanical Engineering

2016

Experimental Evaluation and Thermodynamic System Modeling of Thermoelectric Heat Pump Clothes Dryer

Viral K. Patel
ORNL, United States of America, patelvk@ornl.gov

Dakota Goodman
ORNL, United States of America, goodmandk@ornl.gov

Kyle Gluesenkamp
ORNL, United States of America, gluesenkampk@ornl.gov

Anthony Gehl
ORNL, United States of America, gehlac@ornl.gov

Follow this and additional works at: http://docs.lib.purdue.edu/iracc

Experimental Evaluation and Thermodynamic System Modeling of Thermoelectric Heat Pump Clothes Dryer

Viral K. PATEL*, Dakota GOODMAN, Kyle GLUESENKAMP, Anthony GEHL

Oak Ridge National Laboratory
Oak Ridge, TN, USA
patelvk@ornl.gov, goodmandk@ornl.gov, gluesenkampk@ornl.gov, gehlac@ornl.gov

*Corresponding Author

ABSTRACT

Electric clothes dryers in the US consume about 6% of residential electricity consumption. Available electric clothes dryers today are either based on electric resistance (low-cost but energy-inefficient) or vapor compression (energy-efficient but high-cost). Thermoelectric dryers have the potential to alleviate the disadvantages of both through a low-cost, energy-efficient solution. This paper presents experimental results and steady state simulation of a prototype thermoelectric dryer. A thermoelectric model is coupled with a psychrometric dryer system model to design the experimental prototype. The results from the prototype are used to calibrate the model and identify important parameters that affect performance, such as relative humidity of air leaving the drum.

1. INTRODUCTION

Approximately 80% of households in the US have a clothes dryer and 30% of these are at least 10 years old (EIA, 2009). Typical dryers use a tumble-type drum with air pushed through by a blower to dry clothes. The state of the art includes electric resistance (ER) dryers with once-through air flow, condensing dryers with closed-loop air flow, and vapor-compression (VC) heat pump dryers with closed-loop air flow. Of these, the VC heat pump dryers are most energy-efficient. Although they are based on mature technology and are used extensively in Australia and Europe, they have had poor market penetration in the US, with the major barriers being high cost and longer dry times (Denkenberger, et al., 2013). There is therefore a significant potential for advanced clothes dryers to provide energy savings over standard ER models (York, et al., 2015).

Despite this, research efforts in new and alternative advanced clothes drying technology is relatively limited. Some studies have been performed on understanding and further improving the efficiency of condensing dryers. Condensing dryers typically use an air-to-air heat exchanger to dehumidify the air from the dryer. Because some models are ventless, installation is easier than conventional vented ER dryers. A pertinent example of work in this area is by Cochrane *et al.* (2009), who proposed that surface tension elements (STE) be used to replace the air-to-air plate heat exchanger condensing surface in the dryer. The objective was to use the STE configuration to enhance dehumidification compared to the conventional heat exchanger condensing surface and reduce overall energy consumption. An analytical model was first developed to predict vapor removal from the STE. An experimental prototype was then constructed based on the results of the analytical prediction and implemented into a condensing dryer system. The study showed that in addition to an improvement in the energy efficiency rating, the dryer also operated at a reduced temperature and required less time to dry a given load. Cochrane *et al.* concluded that optimization in the analytical model and incorporation into condensing dryers would further reduce residential energy consumption.

Do *et al.* (2013) conducted an experimental study to fully characterize the performance of a condensing dryer with an air-to-air heat exchanger. They evaluated energy consumption of a closed-loop tumbler dryer as a function of the electric resistance heater capacity, drying air flow rate, cooling air flow rate, dry time and water condensation rate. The parametric study showed that the larger heater power produced shorter dry times, higher air temperature and higher water condensation rates. However, the drying air flow and cooling air flow did not significantly affect the drying performance.

Other research in advanced clothes dryers has been conducted by Bansal *et al.* in modeling (2010a) and experimental development (2010b) of a novel dryer based on a heat exchanger using hot water (potentially sourced from process heat of external combined heat-and-power plants) as the medium. For the experimental development, a conventional once-through dryer was modified by replacing the electric resistance element with a water-to-air finned tube heat exchanger. The experimental performance of the modified and unmodified dryer was evaluated for the same operating conditions. Their new dryer concept was found to have shorter dry times (of 15-18 min) with lower moisture extraction rates for the same total power input, resulting in energy efficiency improvement of up to 11% compared to the conventional unmodified electric resistance dryer.

In vapor-compression heat pump dryers, the heat pump is a refrigeration loop which includes a compressor, evaporator, condenser and expansion valve. In closed-loop systems, air circulates through the loop continuously. VC heat pump dryers are efficient because they use the evaporator to condense moisture from the humid air leaving the dryer drum, and the condenser to heat up the dried air before it re-enters the drum. However, they involve a complicated mechanical system with a secondary heat transfer fluid. Thermoelectric (TE) elements on the other hand are a purely solid-state heat pump technology consisting of two distinct semiconductors sandwiched together in a thin layer. When a DC current is applied, a temperature difference is created between the two sides of the element (Rowe, 1995), and the TE can be used as a heat pump. In the context of clothes dryers, the cold side of the TE elements can be used to condense moisture from the humid air leaving the dryer drum, and the hot side can be used to re-heat the dried air before it re-enters the dryer drum. This can allow for the development of a new type of heat pump clothes dryer with less moving parts compared to VC heat pump dryers, and without any refrigerant.

Considering the above, the research in this paper has two primary objectives. The first is to present a novel energy-efficient thermoelectric clothes dryer as a possible cost effective alternative to existing electric resistance and vapor-compression heat pump dryers. The second is to provide new information in the literature about advanced solid-state heat pump clothes dryer technology, through a combined modeling/experimental study. This includes performance characterization, determination of energy factor and drying time and identification of important parameters that affect overall performance.

2. EXPERIMENT DESIGN AND SETUP

2.1 Prototype dryer setup

The experimental design of the prototype thermoelectric clothes dryer was based on a steady-state, system level, coupled psychrometric and thermoelectric model which was developed in Engineering Equation Solver (EES). The model allows for calculation of the thermoelectric dryer energy factor (EF) and expected dry time for a compact (bone-dry weight of 3.00 lb) DOE load of fabric as described in 10 CFR 430 (2013). The model outlines constraints for the design of the thermoelectric module (described below), such as cooling capacity, leaving hot air temperature, leaving cold air temperature, maximum physical size and pressure drop. This information led to design and fabrication of the TE module, which was then installed in the experimental prototype thermoelectric clothes dryer.

The prototype was a modified donor electric resistance dryer. The electric resistance elements were removed and thermoelectric modules were installed. All controls and switches on the donor dryer were deactivated. Since the donor dryer was vented, the duct work was re-routed so that the blower recirculated the air through the drum rather than exhausting out the back. Figure 1 shows a schematic illustrating pertinent state points in the thermoelectric clothes dryer (left) and a photo of the fabricated experimental prototype (right).
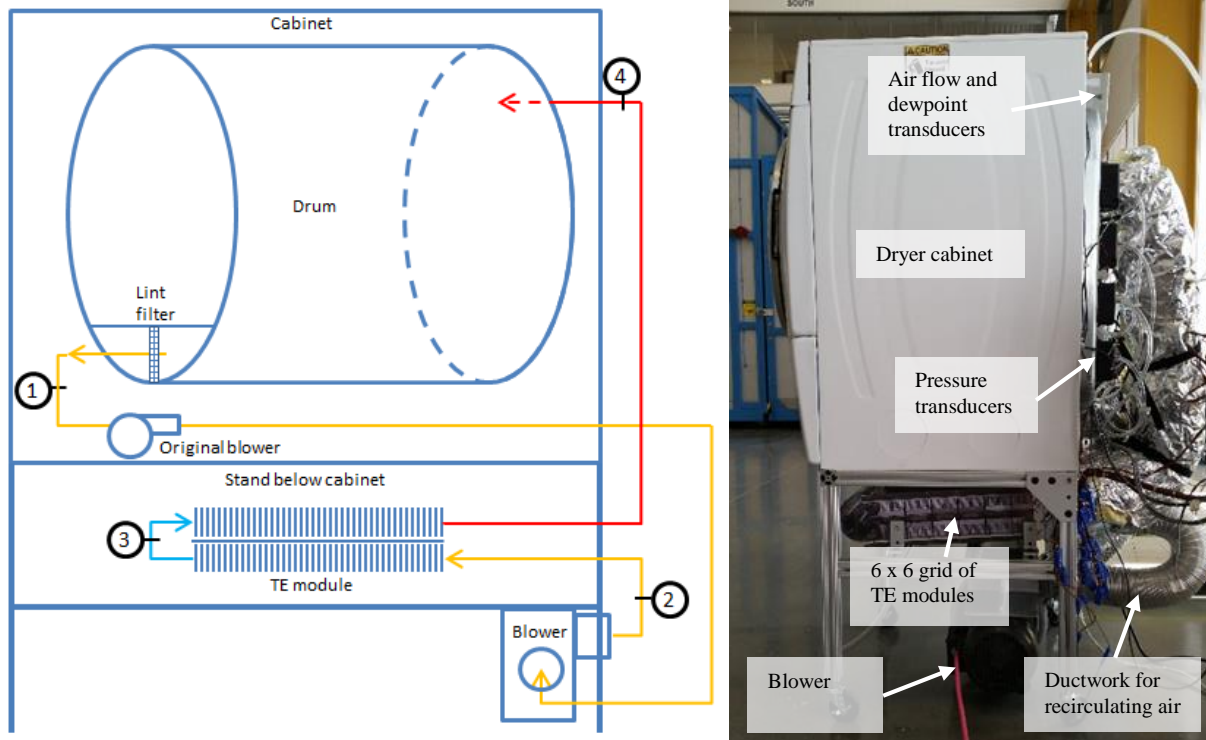
Figure 1: Schematic with state points labeled (left) and photo of fabricated thermoelectric dryer prototype (right)

The order of the state points and arrows in Figure 1 indicate the direction of air flow through the cycle. Pressure transducers were installed at points [1-4] to measure the static pressure in the ducts relative to ambient. A traversing pitot station was installed at point [4] to measure the air flow rate through the cycle. T-type thermocouple probes were installed at points [1-4] to measure air temperature. Dewpoint sensors were installed at points [1], [3] and [4], which (along with corresponding dry bulb air temperatures) allowed the relative humidity to be determined at these points. A new blower was installed in the prototype to allow flexibility in flow rates. This was used in series with the original blower (which was on a common shaft with the drum rotation belt drive).

2.2 Thermoelectric module

The thermoelectric module for the prototype dryer was made up of unit engines which consisted of a thermoelectric element sandwiched between two aluminum pin-fin heat sinks and an aluminum spacer block which acted as a standoff. Off-the-shelf thermoelectric modules were selected for the initial prototype (Thermonamic, 2015). The performance of these modules was measured using a custom evaluation stand. The measured performance was then matched in a model and the resulting TE parameters were used in the design model. This design model was used to devise a design consisting of a 6 x 6 array of thermoelectric elements (total of 36). The 6 x 6 array was designed for a cooling capacity of 1 kW. On the hot side, it was designed to heat air from 35°C to 57°C. A spacer (41mm x 41mm x 15mm) was provided between each TE module and its cold sink.

As shown in Figure 2, the TE modules were sub-divided into 3 banks of 12 thermoelectric elements each. Each bank had a dedicated DC power supply and the elements within a bank were connected in series. Each unit engine in the above 6 x 6 grid was assembled individually and all mated surfaces were coated with a heat sink compound to minimize contact resistances. The unit engines were then installed on a polycarbonate mounting plate and wired according to their bank and dedicated power supply. The hot side of the thermoelectrics faced up and the cold side faced down. Liquid that condensed on the TE cold side was removed from the heat sinks by gravity. When assembly of the 6 x 6 array was complete, the mounting plate slid into a clear housing (labeled "6 x 6 grid" in Figure 1)Figure 1. For airflow, the housing had an inlet and outlet on one end, and a 180° bend on the other. Air flowed as follows through the TE module: inlet → TE cold side heat sinks → 180° bend → TE hot side heat sinks → outlet.

3. MODEL DEVELOPMENT

3.1 Further development of initial model

In addition to the design model used for the experimental prototype design, a separate controls model followed a similar structure and was developed based on initial experimental results from the prototype. Parameters were empirically calibrated for approach temperatures (AT), overall heat transfer coefficient (UA), and relative humidity (RH) on the condensing side of the thermoelectrics. Figure 2 shows the process schematic used in the most recent iteration. State points [1–4] are shared with the design model and Figure 1, while state points [5–9] were added to capture effects of each TE bank. Each of the state points [5–9] is defined (a) on the air side for the psychrometric state leaving each bank and (b) for each TE bank's heat sinks.
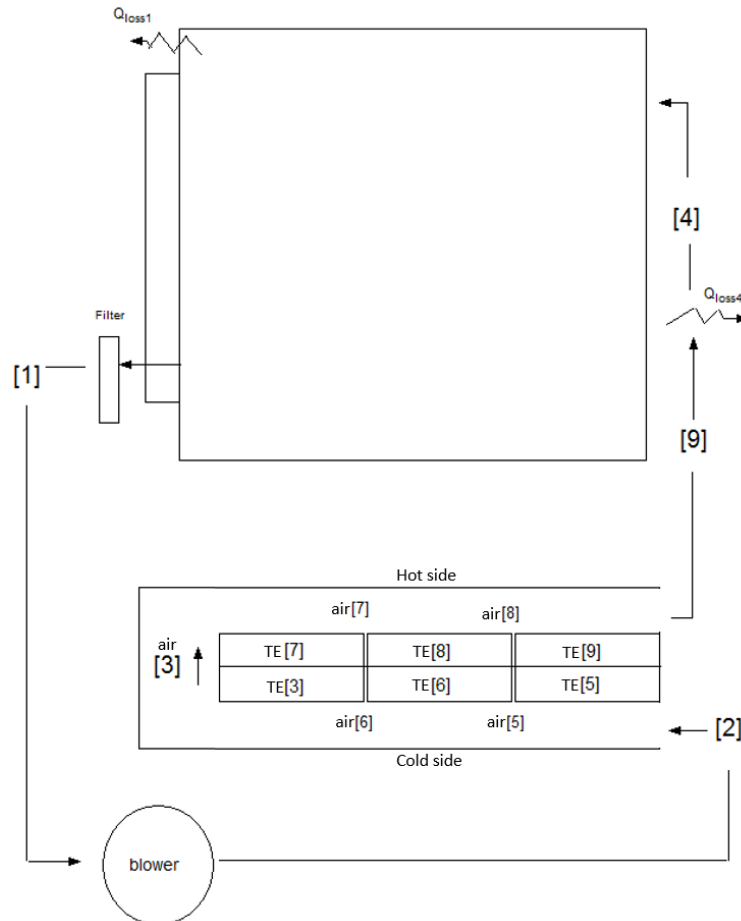
Figure 2: Schematic of thermoelectric dryer model showing state points

During operation, humid air leaves the drum (after gaining moisture from wet fabric) and passes through the lint filter to reach point [1]. It flows through the blower and enters the cold side of the TEs at point [2]. The TE grid is divided into three banks: referring to the labels in Figure 2, the [5] is the cold side of one bank corresponding to [9] on the hot side; and similarly for the second bank (state [6] and [8]) and third bank (states [3] and [7]). As air flows over the cold sinks it is dehumidified as condensation occurs. The air then makes a bend at point [3] and flows over the hot sinks. Sensible heating of the air occurs and it exits the TE duct. Between state [9] and [4], an empirical heat loss parameter accounts for system energy losses in order to ensure an energy balance in the steady state model. The hot, dry air re-enters the drum at point [4], becomes humidified by passing over the moist cloth, and the cycle is complete.

3.2 Calibration

The thermodynamic model was calibrated by tuning a set of parameters to match their experimentally observed values. The calibration parameters fall into two categories: those that were maintained at a constant value across trials, and those that were varied for each trial. Each of these is described briefly below.

Values calibrated and globally applied to all trials (see Table 1):

- AT[3], AT[5–9]: Approach temperatures: how closely the air temperature approached the sink temperature.
- $UA_{loss}[1]$, $UA_{loss}[4]$ (corresponding to the Q_{loss} terms at state points [1] and [4]): to maintain a system-wide steady state energy balance, empirical thermal losses were applied proportionally to the temperature difference between these two state points and ambient.
- RH[3], RH[5], RH[6]: The RH of air leaving each of the three cold banks
- Thermoelectric materials: thermoelectric performance is captured by the model proposed by Goldsmid (1995). Empirical parameters are the thermophysical properties of the thermoelectrics themselves, and good agreement was found with the manufacturer data (Thermonamic, 2015).

Values calibrated and individual applied to each trial (see Table 2)

- Starting and final moisture content (SMC and FMC)
- Bone dry weight (BDW) of cloth load
- Air flow rate
- Mean electrical current applied to TEs

Two additional model calibration parameters were the RH exiting the drum and the electrical resistance of TE elements.

- The RH exiting the drum was modeled based on linear regression to drum entering temperature based on experimentally measured values.
- The electrical resistance of TE elements was modeled based on linear regression to TE hot and cold side temperature, based on experimentally measure values.

Table 1: Calibrated values used for all trials

Parameter	Calibration value
AT[3]	3.0 K
AT[5]	1.0 K
AT[6]	3.0 K
AT[7]	2.0 K
AT[8]	4.0 K
AT[9]	8.0 K
$UA_{loss}[1]$	0 W/K
$UA_{loss}[4]$	29 W/K
RH[3]	0.80
RH[5]	0.60
RH[6]	0.65

Note that each approach temperature in Table 1 corresponds to the state points in Figure 2 as follows:

$T_{TE}[i] = T_{air}[i] + AT[i]$ (hot side, [7], [8], and [9])

$T_{TE}[i] = T_{air}[i] - AT[i]$ (cold side, [5], [6], and [3])

Note also that the UA_{loss} corresponds to the state points in Figure 2 as follows:

$Q_{loss}[i] = UA_{loss}[i]*(T_{air}[i] - T_{ambient})$

Table 2: Measured calibration values specific to each trial

| Parameter	Experimentally measured value								
	Trial 3	Trial 4	Trial 5	Trial 6	Trial 8	Trial 9	Trial 10	Trial 11	Trial 12
SMC FMC	57.5% 4.4%	57.5% 4.3	57.2% 2.8%	57.6% 3.6%	57.6% 1.8%	57.6% 3.56%	57.5% 1.5%	57.8% 2.5%	57.6% 3.65%
BDW [lb]	3.00	3.00	3.00	8.45	3.00	3.00	3.00	8.45	8.45
Air flow rate [CFM]	100	100	115	115	115	115	115	115	115
Electrical currents for TE banks 1, 2, and 3 [A]	1.59 1.47 1.18	2.27 2.35 2.05	2.27 2.38 1.58	2.18 2.44 2.59	2.11 2.18 2.43	2.55 2.18 1.52	2.06 2.05 1.63	2.49 2.28 1.99	1.47 1.47 1.50

4. RESULTS AND DISCUSSION

Several experimental trials were conducted on the prototype TE dryer. The main variation from one trial to another was the electrical current applied to the TE banks. Additionally, variations were made in air flow rate and test load size. The comparison between modeled and experimental values of thermoelectric DC power consumption and total dry time are shown graphically in Figure 3.
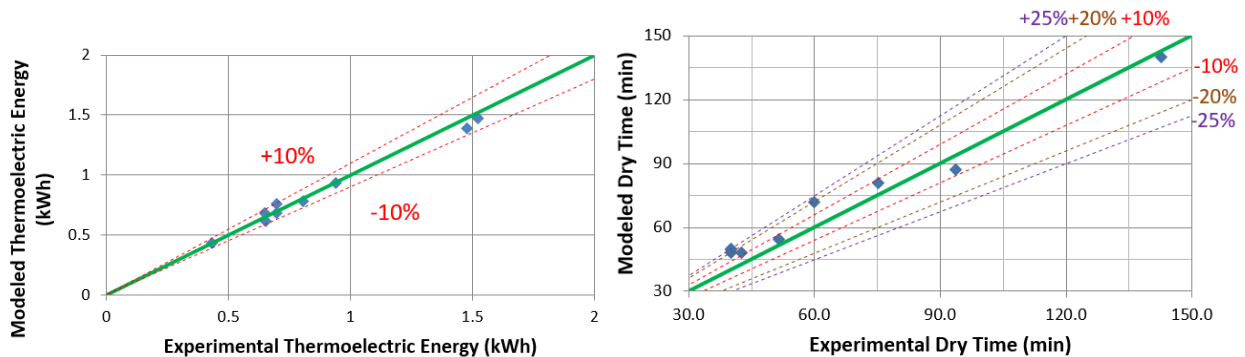
Figure 3: Comparison between experimental and model predicted thermoelectric energy use (left) and dry time (right) for 9 trials

The deviation between experimental and model-predicted thermoelectric energy use is within ±10%. This is an important result because unlike other energy usage in the system which does not vary greatly (i.e. blower and drum motor energy usage), the thermoelectric energy consumption depends on many factors such as the current and temperature difference. During a given test, the temperatures on the hot and cold sides of the TE change with time as the fabric is dried. The dry time is also an important metric; it is closely tied to the energy consumption and accurate prediction via modeling is essential. The results show that model prediction of dry time is within ±25% of experiments.

The modeling and experimental results also revealed that the relative humidity of the air exiting the dryer drum and temperature of the air entering the drum were key factors in the overall performance of the system. The best results were expected from high RH leaving the drum since that means (i) the vaporization of the moisture on the cloth was maximized for a given temperature and (ii) less heat needed to be removed from the air before the onset of condensation. The temperatures also played a large role in the thermoelectric efficiency since the thermoelectric COP worsens at higher temperature lifts. In Figure 4 it can be seen that the model could accurately predict the RH of the air exiting the drum by ±10% and the maximum deviation in drum inlet temperature was within ±5°C.
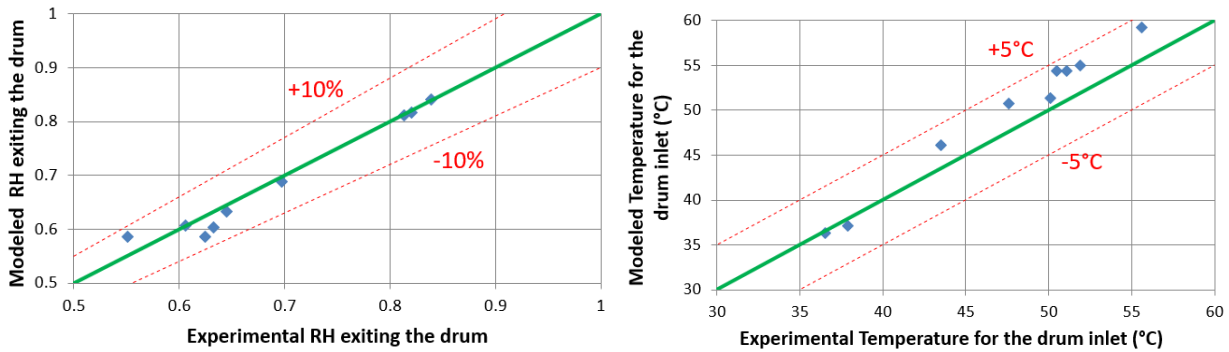
Figure 4: Comparison between experimental and model predicted RH exiting the drum (left) and temperature of air entering the drum (right) for 9 trials

Finally, to compute an EF, the bone dry weight (in lb) of the cloth was divided by the energy used during the drying process (in kWh). This energy included the AC electrical energy consumption of the thermoelectric power supply, the blower, and the drum motor. Power to the thermoelectrics was supplied by DC power supplies that allowed for precise control and measurement. A conversion efficiency of 90% was assumed to account for AC to DC conversion losses. The drum motor power was calculated by using the measured torque required to turn the drum time rotational speed (a constant 37.4 W) divided by an assumed motor efficiency of 60% (for constant 62 W electrical). The blower power was determined from the measurement of flow work done by the blower on the air (i.e. the product of the measured pressure drop and volumetric flow rate), divided by the assumed fan efficiency of 17% and motor efficiency of 60%. The trials conducted so far reached an EF of 4.9, and the maximum deviation between model and experiment was <15% for all trials.

4. CONCLUSIONS

A preliminary experimental and modeling study of thermoelectric clothes dryer was conducted. The results indicate that not only is this novel technology viable for clothes drying, it also can be captured by the model proposed in this work. The results also show that parameters such as the relative humidity and air temperature at given state points are key factors in the overall performance of the system.

ACKNOWLEDGMENTS

REFERENCES

10 CFR 430. (2013). *US Code of Federal Regulations*. Title 10: "Energy"; Part 430, "Energy Conservation Program for Consumer Products"; Subpart B, "Test Procedures"; Appendix D/D1/D2, "Uniform Test Method for Measuring the Energy Consumption of Clothes Dryers".

Bansal, P., Islam, S., & Sharma, K. (2010b). A novel design of a household clothes tumbler dryer. *Applied Thermal Engineering*, 277-285.

Bansal, P., Sharma, K., & Islam, S. (2010a). Thermal analysis of a new concept in a household clothes tumbler dryer. *Applied Energy*, 1562-1571.

Cochrane, M., Goodnight, J., Babin, B., & Eckels, S. (2009). Condensing dryers with enhanced dehudification using surface tension elements. *Applied Thermal Engineering*, 723-731.

Denkenberger, D., Calwell, C., Beck, N., Trimboli, B., Driscoll, D., & Wold, C. (2013). *Analysis of Potential Energy Savings from Heat Pump Clothes Dryers in North America.* Spokane: Ecova, CLASP and SEDI.

Do, Y., Kim, M., Kim, T., Jeong, S., Park, S., Woo, S., . . . Ahn, Y. (2013). An experimental study on the performance of a condensing tumbler dryer with an air-to-air heat exchanger. *Korean Journal of Chemical Engineering*, 1195-1200.

DOE. (2013). *Federal Register: 10 CFR Parts 429 and 430, Test Procedures for Residential Clothes Dryers; Final Rule.* Vol. 78, No. 157: US Department of Energy.

EIA. (2009). *Residential Energy Consumption Survey (RECS).* Energy Information Administration.

Goldsmid, H. (1995). Conversion efficiency and figure-of-merit. In D. M. Rowe, *CRC Handbook of Thermoelectrics* (pp. 19-25). CRC Press.

Rowe, D. M. (1995). *CRC Handbook of Thermoelectrics.* CRC Press.

Thermonamic. (2015). *Specification of Thermoelectric Module TEHC1-19906.* Retrieved from www.thermonamic.com: http://www.thermonamic.com/TEHC1-19906-English.pdf

York, D., Nadel, S., Rogers, E., Cluett, R., Kwatra, S., Sachs, H., . . . Kelly, M. (2015). *New Horizons for Energy Efficiency: Major Opportunities to Reach Higher Electricity Savings by 2030.* Washingston, DC: ACEEE.